AFRL-AFOSR-UK-TR-2012-0012

High Speed Compressor Study

Charles R. Stone

University of Oxford
Department of Engineering Science
Parks Road
Oxford, United Kingdom OX1 3 PJ

December 2011

Final Report for 1 January 2011 to 1 January 2012

Distribution Statement A: Approved for public release distribution is unlimited.

Air Force Research Laboratory
Air Force Office of Scientific Research
European Office of Aerospace Research and Development
Unit 4515 Box 14, APO AE 09421

REPORT DOCUMENTATION PAGE

Form Approved OMB No. 0704-0188

Public reporting burden for this collection of information is estimated to average 1 hour per response, including the time for reviewing instructions, searching existing data sources, gathering and maintaining the data needed, and completing and reviewing the collection of information. Send comments regarding this burden estimate or any other aspect of this collection of information, including suggestions for reducing the burden, to Department of Defense, Washington Headquarters Services, Directorate for Information Operations and Reports (0704-0188), 1215 Jefferson Davis Highway, Suite 1204, Arlington, VA 22202-4302. Respondents should be aware that notwithstanding any other provision of law, no person shall be subject to any penalty for failing to comply with a collection of information if it does not display a currently valid OMB control number.

PLEASE DO NOT RETURN YOUR FORM TO THE ABOVE ADDRESS.

1. REPORT DATE *(DD-MM-YYYY)* 06-Jan-2012	**2. REPORT TYPE** Final Report	**3. DATES COVERED** *(From – To)* 1 January 2011 – 1 January 2012

4. TITLE AND SUBTITLE

High Speed Compressor Study

5a. CONTRACT NUMBER

FA8655-11-1-3032

5b. GRANT NUMBER

Grant 11-3032

5c. PROGRAM ELEMENT NUMBER

61102F

6. AUTHOR(S)

Dr. Charles R. Stone

5d. PROJECT NUMBER

5d. TASK NUMBER

5e. WORK UNIT NUMBER

7. PERFORMING ORGANIZATION NAME(S) AND ADDRESS(ES)

University of Oxford
Department of Engineering Science
Parks Road
Oxford, United Kingdom OX1 3PJ

8. PERFORMING ORGANIZATION REPORT NUMBER

N/A

9. SPONSORING/MONITORING AGENCY NAME(S) AND ADDRESS(ES)

EOARD
Unit 4515 BOX 14
APO AE 09421

10. SPONSOR/MONITOR'S ACRONYM(S)

AFRL/AFOSR/RSW (EOARD)

11. SPONSOR/MONITOR'S REPORT NUMBER(S)

AFRL-AFOSR-UK-TR-2012-0012

12. DISTRIBUTION/AVAILABILITY STATEMENT

Approved for public release; distribution is unlimited. (approval given by local Public Affairs Office)

13. SUPPLEMENTARY NOTES

14. ABSTRACT

The project examined several means of increasing the operating frequency of cryocoolers, with the goal of increasing the power per unit mass (or volume) of cryocooler compressors. A small increase in spring stiffness can be obtained by improving the design, materials and manufacturing techniques of the mechanical springs (flexures), but the consequent increase in operating frequency is small. The use of an auxiliary gas spring to increase frequency is studied in detail, particularly with respect to the compression losses and clearance seal losses. A gas spring can be used to give a very large increase in compressor operating frequency, but at these high frequencies these losses tend to become large, with a consequent reduction in efficiency. Use of a smaller gas spring, with lower losses, but a reduced increase in frequency, will provide a better design for most applications. A design method is described for the embodiment of a gas spring, and a worked example is given, showing how the power output of a particular compressor can be doubled, with a 40% increase in compressor size, and a much smaller increase in mass.

15. SUBJECT TERMS

EOARD, Cryocoolers, Thermodynamics, Thermophysics

16. SECURITY CLASSIFICATION OF:			**17. LIMITATION OF ABSTRACT**	**18, NUMBER OF PAGES**	**19a. NAME OF RESPONSIBLE PERSON** Brad Thompson
a. REPORT UNCLAS	**b. ABSTRACT** UNCLAS	**c. THIS PAGE** UNCLAS	SAR	47	**19b. TELEPHONE NUMBER** *(Include area code)* +44 (0)1895 616163

Standard Form 298 (Rev. 8/98)
Prescribed by ANSI Std. Z39-18

High Speed Compressor Study

Final Report

AUTHORS:	Paul Bailey, Mike Dadd, Richard Stone Cryogenic Engineering Group Department of Engineering Science University of Oxford
REPORT FOR:	USAF AFRL
CONTRACT:	FA8655-11-1-3032
PRINCIPAL INVESTIGATOR:	Richard Stone
DATE:	21-Dec-2011
ADDITIONAL DOCUMENTS:	None
NUMBER OF PAGES:	45
OUR REF:	HS-FR1
PERIOD OF PERFORMANCE:	1st Jan 2011 to 31st Dec 2011

Oxford University
Department of Engineering Science

Distribution A: Approved for public release; distribution is unlimited.

Contents

1 Summary 4
2 Background 4
3 Compressor Operating Frequency: Survey Data 5
4 Compressor Operating Frequency: Resonance 8
5 Mechanical Springs 8
  5.1 Design Criteria 8
  5.2 Mechanical Springs – Stress Analysis 9
  5.3 Mechanical Springs – Material 14
  5.4 Mechanical Springs – Fabrication and Surface Treatment 15
  5.5 Mechanical Springs – Summary 16
6 Gas Spring Stiffness 16
7 Auxiliary Gas Spring - Introduction 17
  7.1 Gas Spring Sizing 19
  7.2 Gas Spring Losses. 20
  7.3 Seal Losses 26
  7.4 Gas Spring Pressures & Stiffness 26
8 Gas Spring: Worked Example 28
  8.1 Basis for calculation 28
  8.2 Calculation Method 29
  8.3 Other Design Considerations 30
  8.4 Simulation Results 32
  8.5 Summary of Simulation Results 37
9 Conclusions 38
10 Acknowledgments 39
11 Appendix A. Cryocooler Frequency Data 40
12 Appendix B. Estimation of Gas Spring Piston Moving Mass 41
13 REFERENCES 45

List of Figures

Figure 1. Cryocooler Operating Frequencies.. 6

Figure 2. Equivalent Beam 9

Figure 3. Spiral Flexure 9

Figure 4. Spiral Spring. The clamp areas are coloured. 10

Figure 5. Von Mises stress in a single arm of a spiral spring............................... 11

Figure 6. Stress at the ‘tear drop' defining the end of a spring arm.. 13

Figure 7. Compressor with auxiliary gas spring. 18

Figure 8. Typical ‘*P-V* ’ Loops.. 19

Figure 9. Loss term as a function of Peclet number. 22

Figure 10. Deviation between the “*y* ” term of the Kornhauser equation and the inverse square approximation over the range 10 < Pe 10000............... 24

Figure 11. Nomenclature for the cylinder surface area... 25

Figure 13. Gas Spring gross and net power, and losses, as a function of End Clearance (gas spring piston diameter = 60 mm)................................. 33

Figure 12 Gas Spring Characteristics as a function of End Clearance (gas spring diameter = 60 mm). 33

Figure 14. Resonant Frequency and gas spring mass as a function of Gas Spring Piston Diameter (End Clearance = 70). 34

Figure 15. Gas Spring gross and net power, and losses, as a function of Gas Spring Piston diameter (gas spring end clearance = 60 mm)................ 35

Figure 16. Net Power and Gas Spring Efficiency as a function of Gas Spring Piston Diameter and End Clearance. 36

Figure 18. Model for Gas Spring Piston mass estimate 42

Figure 17. Typical FE output from piston analysis.. 42

Figure 19. Mass of gas spring piston as a function of piston diameter and gas spring pressure amplitude.. 43

1 Summary

This report describes various techniques for increasing the operating frequency of cryocoolers, with the goal being to increase the power per unit mass (or volume) of cryocooler compressors.

A small increase in spring stiffness can be obtained by improving the design, materials and manufacturing techniques of the mechanical springs (flexures), but the consequent increase in operating frequency is small.

The use of an auxiliary gas spring to increase frequency is studied in detail, particularly with respect to the compression losses and clearance seal losses. A gas spring can be used to give a very large increase in compressor operating frequency, but at these high frequencies these losses tend to become large, with a consequent reduction in efficiency. Use of a smaller gas spring, with lower losses, but a reduced increase in frequency, will provide a better design for most applications.

A design method is described for the embodiment of a gas spring, and a worked example is given, showing how the power output of a particular compressor can be doubled, with a 40% increase in compressor size, and a much smaller increase in mass.

2 Background

The “Oxford” type of flexure bearing/clearance seal cryocooler has a heritage that dates back to about 1980. These early cryocoolers operated at about 40 Hz, and machines to this basic design are still being manufactured. Improvements in design, notably by Northrop Grumman (NG), Oxford University and others have produced a significant increase in operating frequency, and a parallel improvement in specific mass (Watts of cooling per kg).

Recent developments have led to a requirement for smaller, lower cost cryocoolers that can be manufactured in higher quantities and deployed with short lead times.

The size and mass of a cryocooler is determined largely by the compressor, and the primary function of this is to convert electrical power into the Pressure-Volume (*P-V*) power required by the thermodynamic processes in the cold head.

The power delivered by a compressor piston to the gas can be approximated by

$$Power = k\, f\, \Delta P\, \Delta V \qquad (1)$$

Where f is the operating frequency, ΔP is the pressure swing, and ΔV is the swept volume and k is a constant which represents the shape of the “*P-V* ” loop.

If a reduction in overall size is required, the following paths must be followed:

- Design for the maximum ΔV within the overall envelope.
- If a further reduction in volume is needed, then the possibility of increasing ΔP and the operating frequency should be investigated.

The pressure swing in a compressor is largely a function of fill pressure, assuming that the 'working' volumes within the system have already been minimised by good thermodynamic design. Increasing fill pressure is straightforward, but the price for this is an increase in thickness (and hence mass and size) of the pressure containment, and this is more significant where flanged and bolted vessels are used. Thicker walls will also lead to higher thermal conduction losses in places where there are high temperature gradients.

Increasing pressure beyond a certain point typically leads to 'diminishing returns'; where increases in efficiency are countered by increasing losses.

Increasing the operating frequency is an obvious means of increasing system power. Historically this was limited by the design of the spiral spring (the flexure), but developments in spring design have made it possible to operate at higher frequencies.

3 Compressor Operating Frequency: Survey Data

Taking data from the 2007 Space Cryocooler Vendor Survey[1], Figure 1 plots operating frequency against input power for the cryocoolers listed in the survey. The data used is tabulated in Appendix 1.

Work on the scaling of Cryocooler compressors[2] showed that the operating frequency, f and "*P-V* " work, W should vary with an arbitrary linear scaling factor K according to the following relationships:

$$f \propto \frac{1}{K} \tag{2}$$

$$W \propto K^2 \tag{3}$$

Combining these relations suggests that the frequency and power should be related by

$$f = \frac{c}{\sqrt{W}} \tag{4}$$

The constant *c* has been evaluated for all of the compressors in the Vendor Survey sample, and the mean value of *c* has been used to plot the "Theoretical" curve, (with the gradient defined as $W^{-0.5}$) in Figure 1. Two further curves are plotted:

- A power-law trend line for the Northrop Grumman compressors
- A power law trend line for all of the other (non-NG) compressors

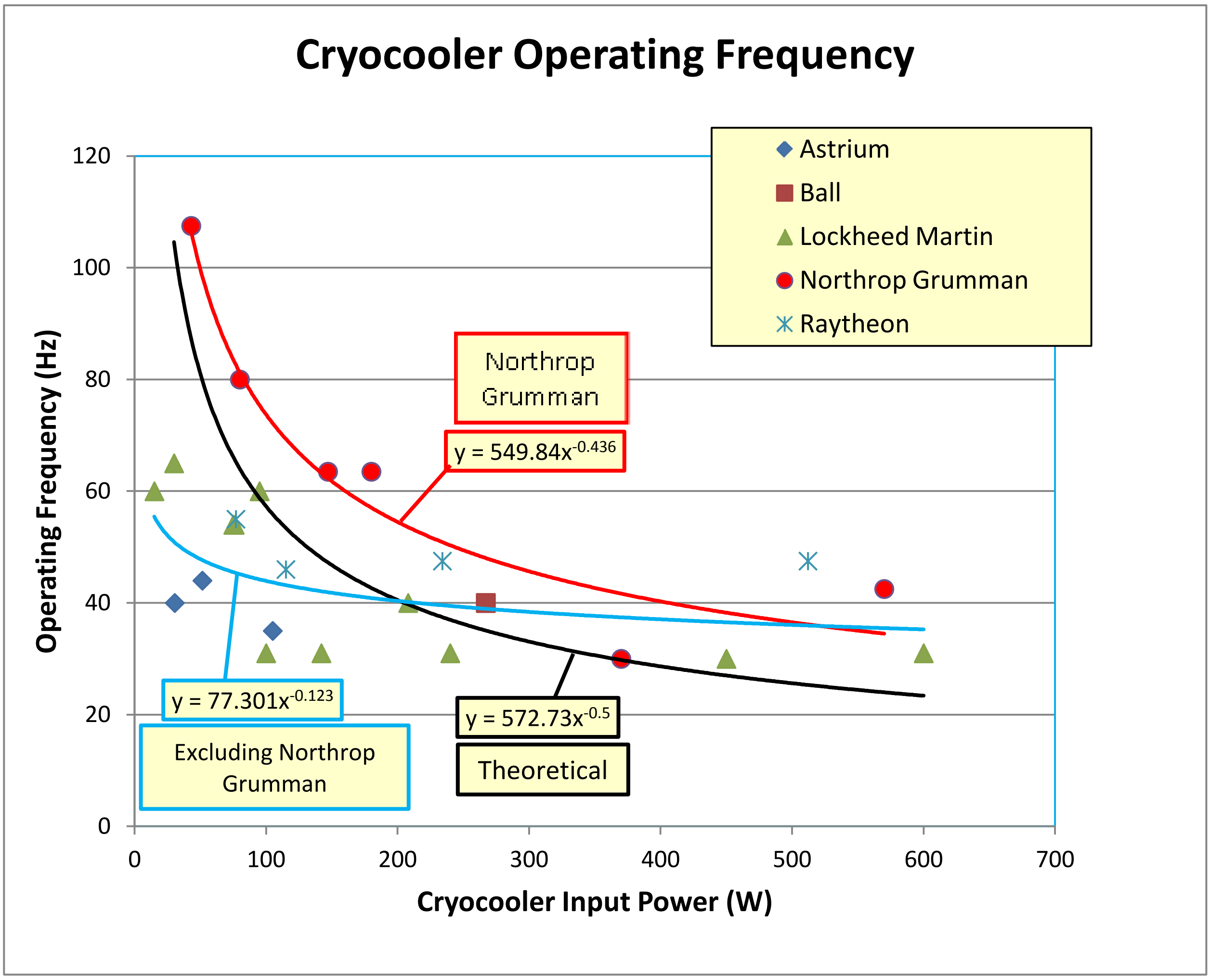

Figure 1. Cryocooler Operating Frequencies.

It can be seen that the NG compressors, which are all based on single design scaled over a range of sizes, give a close approximation to the 'inverse-square-root' law. The non-NG compressors have a much reduced variation of frequency with power, being approximately

$$f \propto \frac{1}{W^{\frac{1}{8}}} \tag{5}$$

This 'scaling' approach is very simplistic and should be treated with caution:

- The data used is from 2007; recent developments are in the direction of smaller and faster compressors[3].
- There are many limitations to the maximum frequency possible in a cryocooler, and some of these are strongly related to the cold end temperature. Examples of such limits are listed below, and some of these are discussed at length later.
  - Heat capacity issues in low temperature regenerators
  - Pressure drop losses
  - Mechanical strength under inertial loading
  - Avoidance of unwanted resonances (for instance, in spring arms)
  - Avoidance of certain frequency ranges (flow-down from satellite requirements)
- The sample includes cryocoolers which operate over a wide range of temperatures, and for thermodynamic reasons there is often a requirement to limit gas velocities in heat exchangers. No allowance is made for this, and it is likely that the NG coolers typically have higher cold end temperatures than the non-NG ones.

However, the one conclusion that should be drawn is that it is clearly possible for most manufacturers to significantly increase the operating frequency of their cryocoolers.

4 Compressor Operating Frequency: Resonance

A cryocooler compressor can be modelled as a classic “mass-spring-damper” system, where the ‘damping’ represents the “*P-V* ” work done on the gas, as well as the various loss mechanisms.

To maximise the motor efficiency, virtually all cryocoolers operate at (or close to) their resonant frequency, which is defined by the spring rate of the system. Typically the spring rate consists of two elements:

- Mechanical Spring stiffness s_m
- Gas Spring Stiffness s_g, which arises due to the effective spring rate when the gas is compressed by the piston in the cylinder.

Hence with an effective moving mass m, the resonant frequency (in Hz) is given by

$$f = \frac{1}{2\pi}\sqrt{\frac{s_m + s_g}{m}} \tag{6}$$

The gas spring rate can be approximated as

$$s_g = A_p^2 \frac{\Delta P}{\Delta V} \tag{7}$$

where A_p is the frontal area of the piston.

It is worth noting that for most compressors, the gas spring stiffness is typically 3 to 4 times the mechanical spring stiffness; the typical spiral flexure does not have high axial stiffness.

To increase the operating frequency of a resonant compressor, it is necessary to increase the total spring stiffness and/or decrease the moving mass.

It has been assumed that any cryocooler already has the moving mass reduced to the minimum that is permitted given the design allowables and margins for the application.

5 Mechanical Springs

5.1 Design Criteria

The mechanical springs (flexures) are a key component in the ‘Oxford’ type of cryocooler. Springs should have a high radial stiffness to maintain the alignment between the piston and cylinder so that there is no contact in the clearance seal.

Typical mechanical springs are designed using the following criteria:

- Size: maximum and minimum diameters for clamping
- High radial stiffness
- High axial stiffness (though this will be orders of magnitude lower than the radial stiffness)
- Maximum stroke
- Peak stress at maximum stroke safely below the 'fatigue limit' for the chosen material
- Avoidance of any undesirable resonances in the spring arms (this limited the maximum operating frequency of early compressors).

5.2 Mechanical Springs – Stress Analysis

A typical spiral flexure is shown in Figure 3, where 6 slots define six spring 'arms' which link the inner and outer clamping areas. Though the exact behaviour of such a spring is complex, a good approximation can be made by assuming that each spring 'arm' acts as a beam 'built-in' at both ends with one end displaced vertically (Figure 2).

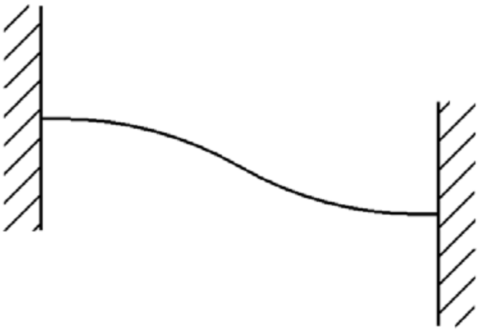

Figure 2. Equivalent Beam

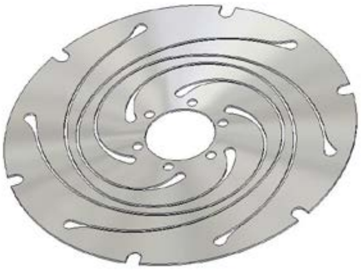

Figure 3. Spiral Flexure

The arguments below are for the deflection of a simple rectangular beam of depth d and breadth b. The mechanical stiffness s_b of a beam of length l, elastic modulus E is given by

$$s_b = 12 \frac{E\, b\, d^3}{l^3} \tag{8}$$

From Figure 2 it can be deduced that the maximum bending moment occurs at the ends of the beam and in the centre it is zero. It is for this reason that the spiral springs arms are typically not of uniform width, but are tapered: thick at the ends, thin in the middle. At the ends of our ideal beam, the maximum bending stress σ for a deflection δ is given as

$$\sigma = k_c \frac{3\,E\,d\,\delta}{l^2} \tag{9}$$

The constant k_c is a stress concentration factor determined by geometry of the spring arm and the clamping arrangement.

A typical spring arm is defined by adjacent slots, and in a good design, these slots are terminated by 'teardrops', whose purpose is to increase the local radius of curvature and decrease the stress concentration. Springs are typically clamped by annular rings at the inner and outer diameters, and the details of any clamp rings, including corner radii and positioning with respect to the 'teardrop' is very significant with regard to the peak stresses that may arise.

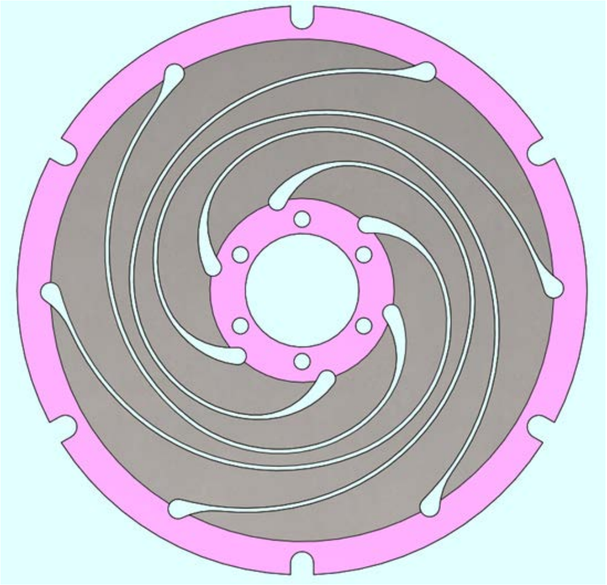

Figure 4. Spiral Spring. The clamp areas are coloured.

A typical clamping arrangement is shown in Figure 4 and the stress distribution in a single spring arm is shown in Figure 5. It can be seen that there are 3 areas of high stress, and two are as predicted by the simple beam theory (at each end of the arm).

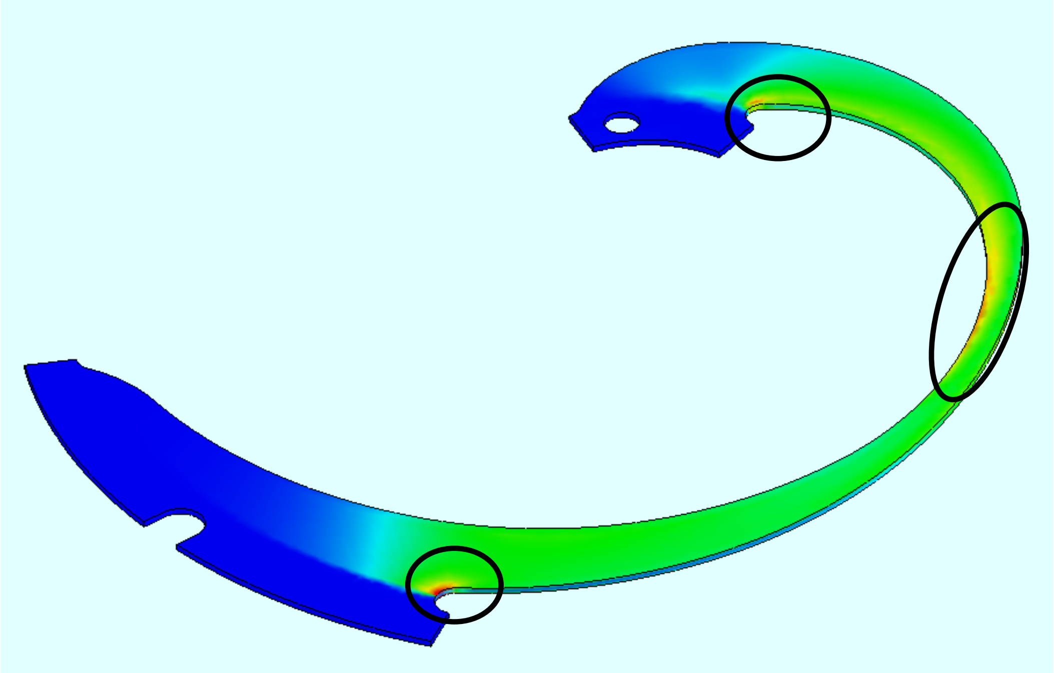

Figure 5. Von Mises stress in a single arm of a spiral spring. Note the three regions of high stress.

The third area of high stress is at the inner edge of the arm, close to the thinnest section, and this is not predicted by the 'simple beam theory'. It can best be understood as follows:

- Consider a simple beam, as in Figure 2 above: as the axial displacement increases, the bending of the beam will give rise to tensile forces within the beam which tend to pull the two 'clamped areas' together – i.e. at right angles to the displacement
- When the 6 'beams' are arranged to form a spiral spring, the summed tensile forces will be equivalent to a torque which will tend to make the inner clamp area rotate with respect to the fixed outer clamp area.
    - To accommodate this, the two spring stacks that typically support the moving parts are aligned with the springs in the same direction, allowing the moving parts to rotate freely. This rotation is small (typically 1° or 2°), and is of no consequence if the piston and cylinder have a circular profile and are mounted concentrically with the springs. (There would be problems if the piston/cylinder were square!) .

- As the spring extends axially, the tensile force in each arm tries to ‘straighten’ each arm in a fashion similar to a ‘Bourdon tube’ in a pressure gauge. This tendency to straighten a curved arm leads to a tensile stress on the inner edge of the arm.
    - Interestingly, this stress does not fully reverse, but varies from (say) +*S* to zero to +*S* as the axial displacement of the spring varies from +*Z* to 0 to *–Z.* This stress varies at double the operating frequency of the compressor.

- In addition to this effect, there is also a double twist in each spring arm. This cannot be seen in figure 5, but it is a real observable effect, and gives rise to higher stresses in the thinnest portion of the spring arm (the same location as the effect just mentioned).

The stress concentration at the outer end of a spring arm is shown enlarged in Figure 6. The clamped area is denoted by the dark blue area (bottom left) bounded by the black curve. It is obvious from Figure 6 that there is a large mismatch between the clamp line, and the geometry of the spring arm. Clamping the spring on an annulus around the outside will inevitably lead to the stress concentration shown in this figure. Changes in the method of clamping, particularly the position of the ‘clamp line’, will greatly reduce the stress concentration in this area.

The argument above has been applied to the clamping at the outer end of the spring arm. A similar argument applies to the inner end of the arm.

With regard to these regions of high stress, the classic engineering goal is for the stress to be equal in all places.

The fatigue life of the spring is determined by the peak stress, and it is clear that if this stress concentration could be drastically reduced, the design could be changed in one or more of the following ways:

- Increasing the spring thickness, which would increase the axial (and radial) stiffness of the spring.

- Decreasing the spring size – the spring outside diameter is often the dimension controlling the diameter of the entire compressor.

- Increasing the stroke, which may improve the motor efficiency and give a higher swept volume.

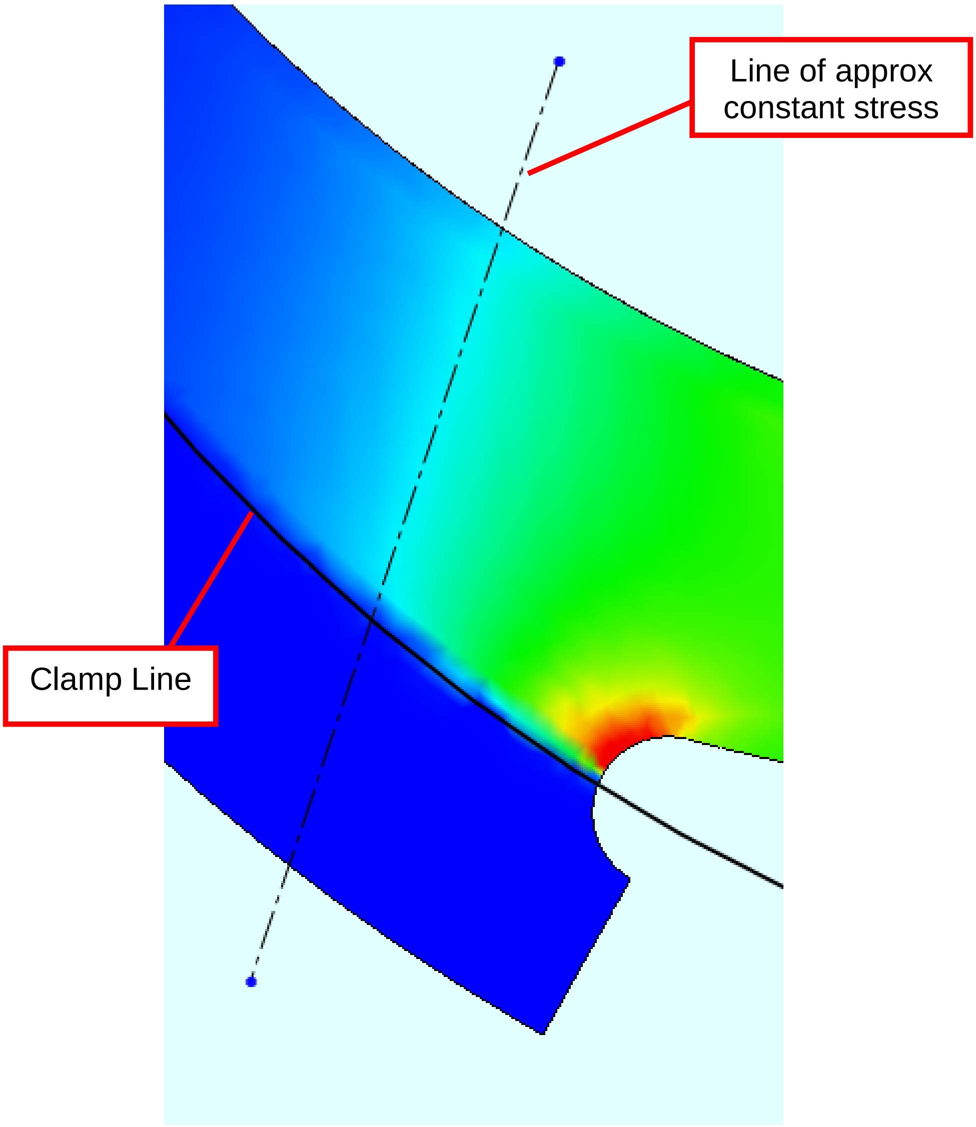

Figure 6. Stress at the ‘tear drop' defining the end of a spring arm. The peak stress is about 865 MPa, compared with 350 MPa across the adjacent part of the arm (a stress concentration factor, $k_c = 2.47$). The clamp line is shown as a solid curved line. A contour of approximately constant stress is shown by the straight chain line.

5.3 Mechanical Springs – Material

In the early cryocoolers, beryllium copper (BeCu) was used for springs, and it is still the material of choice for some manufacturers. Alloys with 1.6 to 2% Be are used, typically to UNS C17000 and C17200. In the full hard condition, the Tensile Strength (UTS) can be as high as 1500 MPa, with a fatigue strength (in reverse bending) in the order of 300 MPa. Despite being non-ferrous, this alloy does have a 'fatigue limit', and is suitable for high cycle fatigue.

Beryllium copper has been largely superseded by stainless steel, which is more readily available 'mill hard' and to the high flatness tolerance which is required for the photo-etching process typically used for spring manufacture.

Stainless steel does have the disadvantage of lower electrical conductivity than BeCu, and there are also issues with surface contact resistance if the material is used as part of the electrical circuit connecting to the moving coil in a typical motor. In terms of physical properties, the ratio of elastic modulus to density (E/ρ) is significantly higher for stainless steels, whose elastic modulus is about 200 GPa compared with about 130 GPa for BeCu; this alone gives a 50% increase in stiffness.

The stainless steel alloys that are typically used are the austenitic grades (AISI 300 series), as these are virtually non-magnetic and hence do not affect the magnetic circuit of the motor, which is typically close to the springs. Fatigue strength of the cold worked alloys are in the region of 400 to 500 MPa, which is significantly higher than BeCu.

There are also some Duplex Stainless steels which have been developed for applications such as the reed valves (flapper valves) used for self-acting (one way) valves in compressors[*]. These have fatigue strengths which are claimed to be in the range of 600 to 800 MPa, which is significantly higher still than austenitic steels. The Duplex stainless steels have the disadvantage of being magnetic, which limits their use to locations where the magnetic field strength is low.

The concept of 'fatigue limit' has been mentioned above. The required lifetime for a space cryocooler is 10 years, which equates to 1.6×10^{10} cycles for operation at 50 Hz, and correspondingly more for higher frequencies (or lifetimes). Carbon fibres and other composite materials have very high fatigue strength, but do not have a 'fatigue limit', and for this reason they cannot be safely used in these applications.

---

[*] Examples are Hiflex, 20C and 7C27MO2 made by Sandvik, and UHB Stainless 716 and 731 made by Uddeholm.

5.4 Mechanical Springs – Fabrication and Surface Treatment

The flat springs used in cryocoolers are typically made by photo-etching, which is a fairly cheap method of manufacture that does not involve high process stresses in the material. Alternative (but more costly) methods are available such a:

- Laser cutting. This does burn the material, so there will be a ‘heat affected zone’ (HAZ) by the cut edge; in practice this should be small.

- Wire Electro-Discharge Machining (EDM, or spark erosion) uses a spark to burn away the edge of the material. There will be also be a HAZ, but the heat input is lower and the effects are less than with laser cutting.

- Water jet cutting is a possibility, but is typically too coarse for the geometry required, especially in small sizes.

- Fine blanking is a method that would be ideal for high volume production, but it is not suited to a spring where narrow slots separate the spring arms (such as shown in Figure 3). Typically tooling costs are very high, but component costs are very low.

A serious issue with the photo-etching process is the macroscopic surface generated by the process. The acid etchant will not act uniformly on the material, but will preferentially etch the boundaries between the grains. The result of this is the creation of many small cracks, all of which can act as initiation sites for fatigue cracks.

Various surface treatments area available which can theoretically improve the fatigue life of the springs, such as:

- Electropolishing – this eliminates ‘high spots’ and provides an improved surface finish, but will have little effect on any deep cracks, such as those etched between grain boundaries.

- Tumbling and shot peening. These techniques are used to improve the fatigue resistance of flapper valves, and the processes essentially put the surface of the component in compression, which inhibits the formation of surface cracks.

The conclusion that should be drawn is that the spring material and method of manufacture should be chosen to optimise the fatigue strength of the part; this is not always done at present.

5.5 Mechanical Springs – Summary

As stated above, the resonant frequency of the compressor is given by

$$f = \frac{1}{2\pi}\sqrt{\frac{s_m + s_g}{m}} \tag{10}$$

where s_m is the axial stiffness of the mechanical spring.

By changing the design of the spring and the material and manufacturing process (especially the finishing) a significant increase in the axial stiffness of a spring can be obtained.

A further gain may also be made by increasing the number of springs used to mount the compressor, providing that there is an overall increase in stiffness per unit of moving mass. (Note that if the springs are very heavy, extra springs may actually reduce the resonant frequency, not increase it).

It is very difficult to quantify the gains that can be made by the various techniques listed above. The end point of the improvement process can be deduced, but there is a wide range of starting points, and due to commercial confidentiality, details of most existing designs are unknown to the authors of this report.

Hence some manufacturers may gain a 100% increase in (for example) spring stiffness by adopting these techniques. Other manufacturers may be doing some of these things already, and will gain less. We are not aware of any manufacturer who is embodying all of the design improvements suggested above.

For a typical cryocooler, the mechanical springs only supply between 1/3 and 1/4 of the total spring stiffness required for resonance, so if the mechanical springs are double the stiffness, the total spring rate will only increase by 25%, giving an increase in resonant frequency of about 12%.

6 Gas Spring Stiffness

From above, the gas spring rate of a piston, compressing gas in a cylinder, can be approximated as

$$s_g = A_p^2 \frac{\Delta P}{\Delta V} \tag{11}$$

Where s_g is the gas spring rate, A_p is the frontal area of the piston, and ΔP and ΔV are the pressure swing and swept volume.

At first glance, the most obvious way to increase the gas spring stiffness is to increase the piston area (i.e. the diameter of the piston) and to decrease the stroke.

With regard to spring design, a small stroke is desirable; within a given diameter, the lower the stroke, the higher the spring stiffness (both radial and axial).

From the point of view of motor design, a large stroke is desirable. This can be explained with regard to the power generated by a linear motor:

$$Power = Force_{rms} \times Velocity_{rms} \qquad (12)$$

With a small stroke, the velocity will be low, and the force required from the motor will be high. Typically, for a moving coil motor, the force is proportional to the current:

$$Force = B\ i\ L \qquad (13)$$

Where the flux density is B, the current i and the effective conductor length L. (Other motor designs, such as moving magnet, will have an equivalent relationship between current and force). The most significant loss in most motors is the loss due to the resistance *R* of the drive coil:

$$Power_{loss} = i^2 R \qquad (14)$$

Hence with regard to 'motor design', there is strong requirement for a high velocity and low force, and in this case the limit is typically the maximum stroke capability as determined by the springs.

Hence with a conventional design, there is a limit to the maximum stiffness of the gas spring effect that can be obtained from the compression process.

7 Auxiliary Gas Spring - Introduction

A possible means of increasing the overall spring stiffness is with the use of an auxiliary gas spring. Such an arrangement is shown in Figure 7.

Auxiliary gas springs need careful design to be effective:

- For a given swept volume, there is an increase in overall size of the compressor.
- There is an increase in moving mass associated with the extra piston. For the auxiliary spring to be effective, there must be an overall increase in spring stiffness per moving mass.

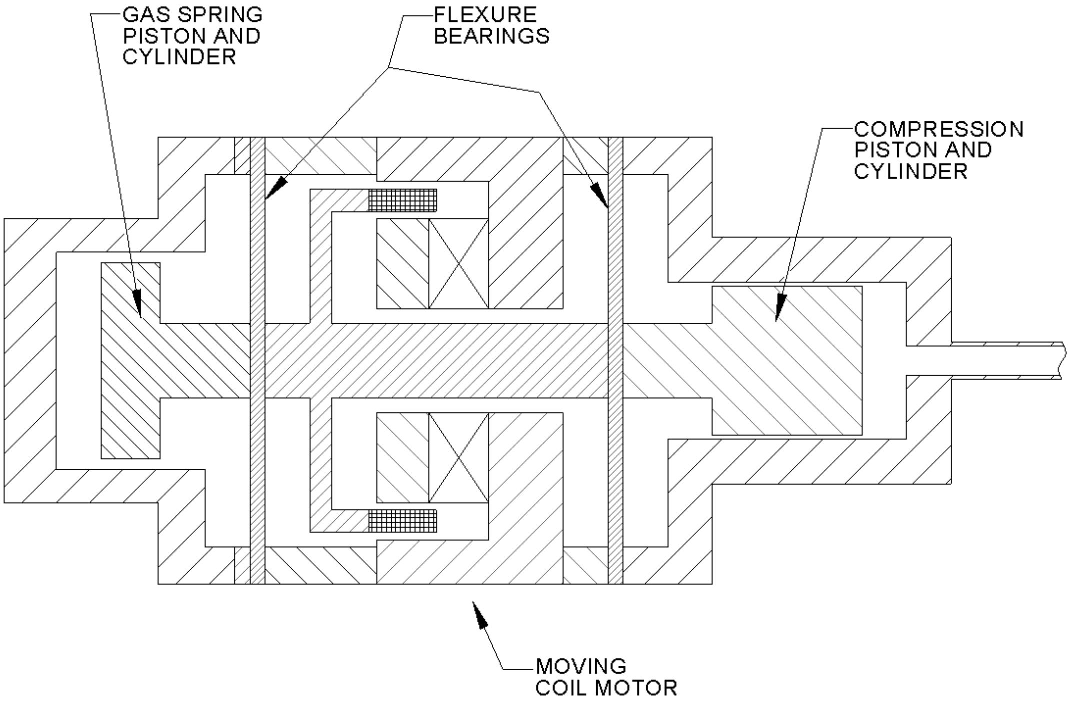
GAS SPRING PISTON AND CYLINDER
FLEXURE BEARINGS
COMPRESSION PISTON AND CYLINDER
MOVING COIL MOTOR

Figure 7. Compressor with auxiliary gas spring.

- There will be thermodynamic losses associated with the gas spring arising from two phenomena:
  - A loss due to flow through the clearance seal between piston and cylinder
  - A 'compression loss' due to irreversible heat transfer in the gas spring.
- There is an issue with linear compressors, usually known as "DC offset" whereby if the mechanical spring rate is relative low compared to the gas spring, gas pressures can cause the mid-point of oscillation to shift away from the 'mechanical zero' as defined by the mechanical springs; a process which can lead to an effective reduction in stroke[4,5]. A poorly designed gas spring could exacerbate this "DC offset" problem. Conversely, the gas spring could be designed in such a way that it completely neutralises the "DC Offset" effect.
- The compressor has more components and the assembly process is more complex. With a gas spring there will be two piston/cylinder combinations to be aligned with the axis of motion of the compressor.
  - The extra complexity is likely to lead to an increase in cost.

- Unless care is taken with the design, assembly methods and fixturing, it may be difficult to achieve alignment required for satisfactory operation of clearance seals.

7.1 Gas Spring Sizing.

From equation (11) above, the stiffness s_g can be re-written in terms of the stroke amplitude:

$$s_g = \frac{A_p \Delta P}{2\, L_a} \tag{15}$$

where A_p is the frontal area of the piston, L_a is the stroke amplitude and ΔP is the pressure swing. The optimum size and aspect ratio should be evaluated with respect to the thermodynamic losses and the piston diameter (and mass) required.

The relationship between P and V is different for the 'compression space' of a cryocooler and for a gas spring (see Figure 8.)

- In a compression space, if there is thermodynamic work being done there will be a significant phase shift between pressure and volume, and the 'P-V' loop will be a fat "blob".
- In a gas spring, hopefully there will be very little work done (if the losses are small), and the "*P-V*" loop will be a thin "sausage".

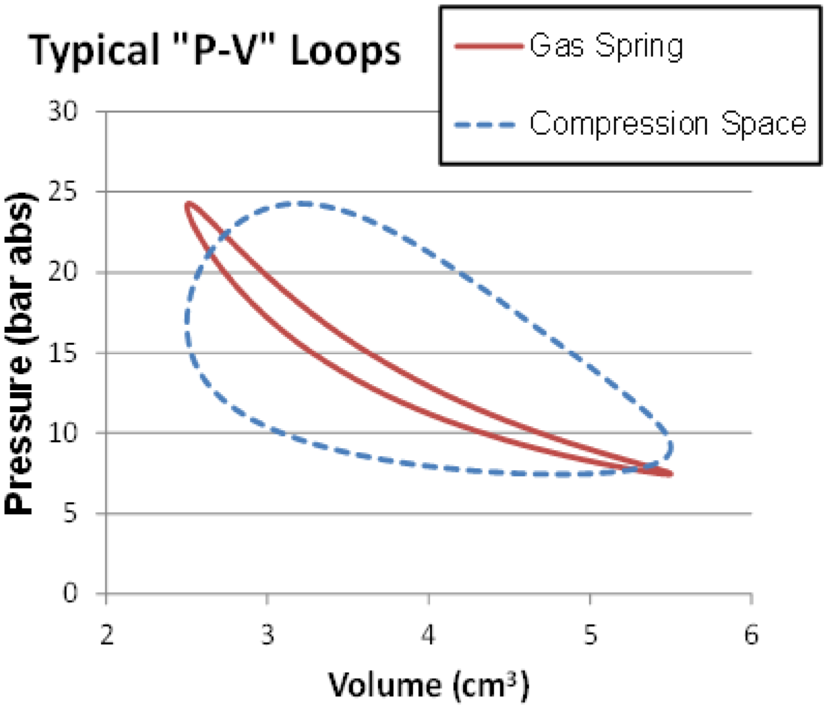

Figure 8. Typical '*P-V*' Loops.

For a gas spring, the end points of the loop (top left and bottom right) can be related by an equation of the form

$$P\,V^n = constant \tag{16}$$

Where n is known as the polytropic index, and is numerically between 1 and γ (the ratio of specific heats). For helium ($\gamma \approx 1.67$), n has been measured in a 'dead volume' test on compressor as being about 1.5. At higher frequencies, the process will tend to become more adiabatic, and so the polytropic index will tend to be higher.

7.2 Gas Spring Losses.

A theoretical expression for the loss in a gas spring was determined by Lee[6] and Cooke-Yarborough[7], and this was modified in the light of experimental work by Kornhauser and Smith[8]. Their experimental data was obtained from a crank-driven compressor, and further experimental work at Oxford[9] verified that Kornhauser's equation was applicable to the linear clearance seal compressors as used in many cryocoolers.

Recently, experimental work and CFD analysis by Lekić[10] has further confirmed the work of Kornhauser, but Lekić has suggested the use of small correction factors in certain ranges. Kornhauser's expression (without Lekić's correction) has been used for the analysis below.

Kornhauser's expression for the gas spring loss is given as

$$E_c = \frac{\pi}{2}\, p_0 V_0 \left(\frac{p_a}{p_0}\right)^2 \frac{(\gamma-1)}{\gamma}\; \frac{1}{y} \left(\frac{cosh(y)\, sinh(y) - sin(y)\, cos(y)}{cosh^2(y) - sin^2(y)}\right) \tag{17}$$

which can be rearranged to give non-dimensional loss term L_{nd} in terms of the Peclet Number:

$$L_{nd} = \frac{E_c}{\frac{\pi}{2}\, p_0 V_0 \left(\frac{p_a}{p_0}\right)^2 \frac{(\gamma-1)}{\gamma}} = \frac{1}{y} \left(\frac{cosh(y)\, sinh(y) - sin(y)\, cos(y)}{cosh^2(y) - sin^2(y)}\right) \tag{18}$$

Where

$$y = 0.49\, Pe_\omega^{0.43} \tag{19}$$

And the Peclet number Pe is given by

$$Pe_\omega = \frac{\omega\, D_h^2}{4\, \alpha_0} \tag{20}$$

$$D_h = \frac{4\, V_0}{A_0} \tag{21}$$

where E_c = Compression loss per cycle

$$E_c = \oint p \, dV \tag{22}$$

p_0 = pressure at mid-stroke
V_0 = cylinder volume at mid-stroke
p_a = pressure amplitude
γ = ratio of specific heats
ω = angular frequency
A_0 = cylinder surface area at mid-stroke
α_0 = thermal diffusivity of gas at mid-stroke, given by

$$\alpha = \frac{k}{\rho \, C_p} \tag{23}$$

Where k, ρ and C_p are all gas properties evaluated at mid stroke and are defined as

k = thermal conductivity
ρ = density
C_p = specific heat at constant pressure

The Non-dimensional loss equation is strongly dependent on the Peclet number; the right-hand side of equation (18) is shown as a function of Pe in Figure 9.

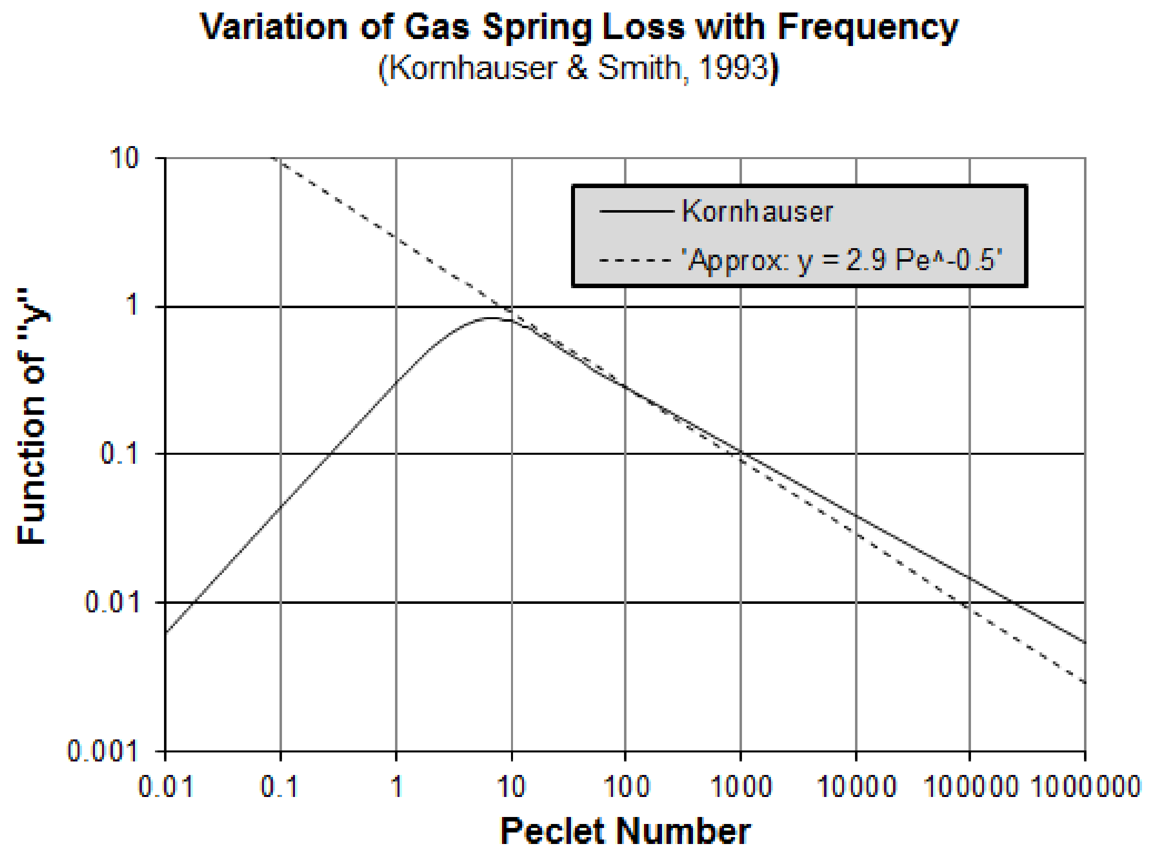

Figure 9. Loss term as a function of Peclet number. An approximation for high Pe is shown with the form $y = A\ \mathrm{Pe}^{-0.5}$

Mathematically, as y increases, $cosh(y)$ and $sinh(y)$ both converge to the same large number, so the cos and sin terms become insignificant, and hence for $y >> 1$

$$\left(\frac{cosh(y)\, sinh(y)}{cosh^2(y)}\right) \approx 1 \tag{24}$$

$$f(y) \approx \frac{1}{y} \tag{25}$$

The odd shape of this function can also be explained with regard to basic thermodynamic processes – the major loss mechanism is heat transfer (between the gas and the cylinder surfaces) across a finite temperature difference. In crude terms this can be explained as follows:

- At low Peclet number (slow speed operation) there is plenty of time for heat transfer, and so the process tends to isothermal; the loss will be low as all of the temperature differences for heat transfer tend to zero.

- At high Peclet numbers there is no time for heat transfer; the process tends to become adiabatic, and though the temperature differences are large, the heat flow is small, so the loss will be small.

Typically the compression space of a cryocooler compressor will operate with Peclet numbers in the range from about 1 to 100, which is the worst possible range for losses. Given that this is an investigation into high speed compressors, we will assume that we are interested in the upper end of this Peclet number range, and hence the equation for the loss reduces to:

$$E_c = \frac{1}{y} \left\{ \frac{\pi}{2} p_0 V_0 \left(\frac{p_a}{p_0} \right)^2 \frac{(\gamma - 1)}{\gamma} \right\} \tag{26}$$

$$E_c = 2.04\, Pe^{-0.43} \left\{ \frac{\pi}{2} p_0 V_0 \left(\frac{p_a}{p_0} \right)^2 \frac{(\gamma - 1)}{\gamma} \right\} \tag{27}$$

In order to illustrate the functional dependence, a further simplification can be made by approximating the function of the Peclet number as an inverse square root law, i.e.

$$f(Pe) = K_p\, Pe^{-0.5} \tag{28}$$

Where K_p is a constant valid for a limited range of Peclet numbers.

This shown in Figure 9, together with the "*y*" term of the full Kornhauser equation. Over the range of Peclet numbers from 10 to 10000, using a value of K_p = 2.95 gives an error in f(Pe) which varies from 0.2% (at Pe = 200) to +/- 20% at the ends of this range (Figure 10). Note that in a real iterative design process, once the Peclet number range is known more precisely, this constant (2.95 in the above approximation) can be adjusted to give a closer fit at the design point. (It should also be noted that if the analysis is done numerically, there is little point in making this approximation, as the function $Pe^{-0.43}$ can be easily calculated).

By using this inverse square term, the equation for the compression loss can be simplified considerably.

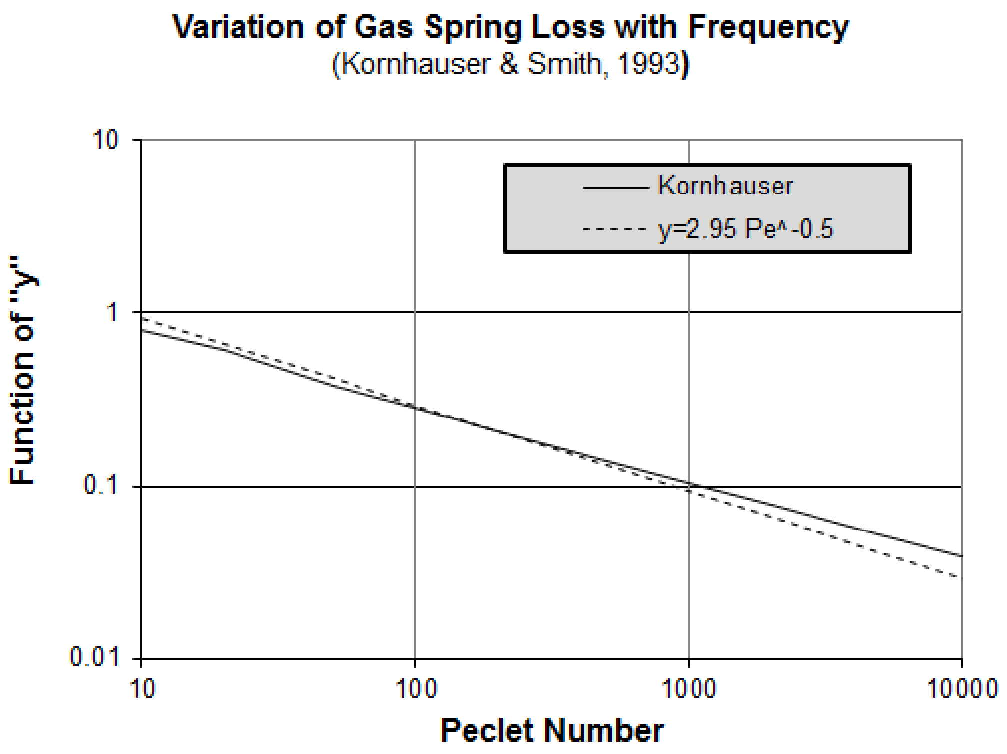

Figure 10. Deviation between the "*y* " term of the Kornhauser equation and the inverse square approximation over the range 10 < Pe 10000

The definition of Peclet number from equations (20) and (21) can be re-arranged as follows

$$\frac{1}{\sqrt{Pe}} = \sqrt{\frac{4\,\alpha}{\omega}\;\frac{A_0^2}{16\,V_o^2}} \tag{29}$$

$$\frac{1}{\sqrt{Pe}} = \frac{1}{2}\sqrt{\frac{\alpha}{\omega}}\;\frac{A_0}{V_0} \tag{30}$$

If the 'inverse square' approximation is applied, then the term above can be substituted into equation (27), and the loss can be expressed as a power (W_c), rather than as energy per cycle (E_c) by multiplying by the operating frequency:

$$W_c \approx \frac{K_p}{2}\;\frac{\omega}{2\,\pi}\;\sqrt{\frac{\alpha}{\omega}}\;A_0\left\{\frac{\pi}{2}\;\frac{p_a^2}{p_0}\;\frac{(\gamma-1)}{\gamma}\right\} \tag{31}$$

$$W_c \approx \frac{K_p}{8}\sqrt{\alpha\,\omega}\;A_0\left\{\frac{p_a^2}{p_0}\,\frac{(\gamma-1)}{\gamma}\right\} \tag{32}$$

Note the following with regard to the above equation:

- The expression applies only for Pe > 10
- The constant K_p gives a close approximation over a limited range of Peclet numbers, but its value can be adjusted to give a better fit for a different range of Pe.
- p_a is the pressure amplitude; p_0 is the pressure at mid-stroke.
- A_0 is cylinder surface area at mid stroke; this will always be larger than A_p the frontal area of the piston.

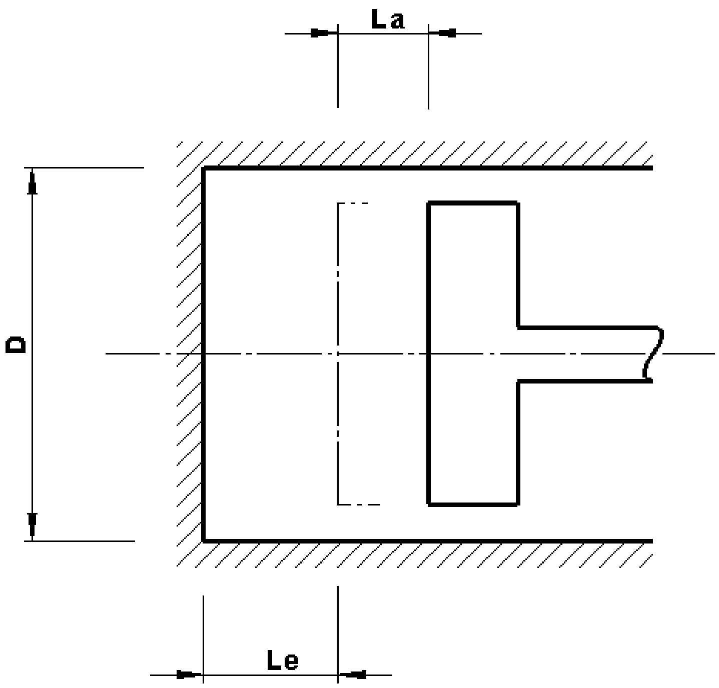

Figure 11. Nomenclature for the cylinder surface area.

Figure 11 shows a gas spring cylinder of diameter D, shaped to be of the simplest geometry. The stroke amplitude of the piston is L_a and there is a clearance length L_e to limit the maximum pressure in the gas spring.

The cylinder surface area at mid-stroke, A_0 is given by

$$A_0 = 2\,\frac{\pi}{4}\,D^2 + \pi\,D(L_a + L_e) \tag{33}$$

$$A_0 = \pi\,D\left(\frac{D}{2} + L_a + L_e\right) \tag{34}$$

7.3 Seal Losses

The power loss due to leakage in a clearance seal, W_s can be approximated as follows[11]

$$W_s = \frac{\pi\,D\,t^3 p_a^2}{24\,\mu\,L_s} \tag{35}$$

D = Seal Diameter
t = Seal radial clearance
p_a = pressure amplitude
μ = Viscosity
L_s = Seal axial Length

Note the following from these approximate loss terms:

- Both the seal loss and compression loss vary with the square of the pressure amplitude (p_a)
- The seal loss is independent of frequency
- The compression loss varies with the square root of frequency

7.4 Gas Spring Pressures & Stiffness

We now have the expressions we need to optimise the gas spring.

From above, the gas spring stiffness can be rewritten as

$$s_g = \frac{\frac{\pi}{4} D^2\,p_a}{L_a} \tag{36}$$

The pressure amplitude can be expressed as a function of the geometry of the piston/cylinder. If the Pressure at Top Dead Centre[†] (TDC) is p_1, then

$$p_a = p_1 - p_0 \tag{37}$$

And p_1 and p_0 are related by a polytropic expression

$$p_1\, V_1^n = p_0\, V_0^n \tag{38}$$

$$p_a = p_0 \left(\frac{V_0}{V_1}\right)^n - p_0 \tag{39}$$

$$p_a = p_0 \left[\left(\frac{V_0}{V_1}\right)^n - 1\right] \tag{40}$$

With the simple geometry shown in Figure 11, the ratio of volumes can be expressed as

$$\frac{V_0}{V_1} = \frac{L_a + L_e}{L_e} \tag{41}$$

$$\frac{V_0}{V_1} = \frac{L_a}{L_e} + 1 \tag{42}$$

Hence

$$p_a = p_0 \left[\left(\frac{L_a}{L_e} + 1\right)^n - 1\right] \tag{43}$$

$$s_g = \frac{\frac{\pi}{4} D^2\, p_0 \left[\left(\frac{L_a}{L_e} + 1\right)^n - 1\right]}{L_a} \tag{44}$$

[†] TDC: in a gas spring this is when the cylinder volume is at a minimum & cylinder pressure at a maximum.

8 Gas Spring: Worked Example

8.1 Basis for calculation

Having derived the equations for a gas spring, it is now possible to determine what a gas spring would look like on a real compressor.

To avoid issues of confidentiality, this exercise has been carried out on a relatively old design of compressor, initially developed for use with a Stirling cycle domestic freezer[12], and subsequently used in a series of experiments on Gas Spring losses9.

Note that this particular compressor is not of modern design, is not compact, but does have reasonably high efficiency (80%).

The original design specification for the compressor (subsequently referred to as the "Ambient Compressor") is as follows:

Table 1. **Ambient Compressor Specification**

Type		Flexure Bearing Clearance Seal
Balance		Single compressor (unbalanced)
Gas		Helium
Piston Diameter	mm	18
Maximum Stroke	mm (peak-to-peak)	12.8
Design Frequency	Hz	50
Effective Moving mass	gram	120
Fill Pressure	bar (abs)	35
Pressure Swing	bar (peak-to-peak)	5.75
Mechanical Spring Stiffness (axial; total)	N/m	3900
Compressor Shaft (P-V) power	W	42.3

8.2 Calculation Method

The design method used is as follows:

- Choose a diameter for the gas spring ("*D*" in Figure 11: range 35 to 80 mm)
- Choose a clearance Length ("L_e" in Figure 11: range 30 to 95 mm)
- Calculate the expected peak-to-peak pressure in the gas spring, and hence the gas spring stiffness.
- Calculate the total spring stiffness for the compressor (compression space + auxiliary gas spring + mechanical springs)
- For the given piston diameter and gas spring pressure swing, calculate the piston mass according to the following empirical formula (derivation of this is given in Appendix 2)

$$m_{gp} = 16 + 1.7 \times 10^{-6}(0.8 + p_a)D^4 \quad (45)$$

Where

m_{gp} = estimated mass of gas spring piston (grams)
p_a = Gas spring pressure amplitude (zero-to-peak) (MPa)
D = Gas spring piston diameter (mm)

- By adding the gas spring piston mass, the total moving mass is found
- From this the resonant frequency is calculated
- Calculate the gas spring compression loss. Note that this is calculated for the gas spring only[‡].
- Calculate the gas spring seal loss
- Assuming the same "*P-V*" work per cycle, calculate the gross "*P-V*" power in the compression space at the revised resonant frequency
- By subtracting the Gas spring seal and compression losses, calculate the Net "*P-V*" work from the compression space which is available for powering a cold head.

This approach gives an 'Upper Bound' to the increase in power capability that can be achieved with a gas spring.

[‡] There is an argument to say that a separate calculation should also be carried out due to the gas spring effect in the gas that surrounds the springs, motor etc. This volume typically has a very small pressure swing, and a very large surface area (the surfaces of the springs, magnetic circuit, moving coil, etc.)

8.3 Other Design Considerations

The reality is that there are several other loss mechanisms, which are not easy to quantify with a simple model of this nature; detailed analysis is beyond the scope of this work. Most (but not all) of these have a negative impact on overall performance.

- **Motor Power.** A simplistic view of the power consumption and motor efficiency as frequency increases follows the following logic:

    - The pressure swing in the compression space remains constant
    - The electromagnetic force delivered by the coil in the air gap remains constant.
    - The current in the coil remains constant
    - If the coil resistance and current remain constant, then the Joule heating of the coil (i^2R) is constant
    - The voltage supplied to the coil must increase proportionally with the piston velocity
    - The useful power delivered by the motor increases proportionally with piston velocity
    - The electromagnetic efficiency of the motor increases, as the Joule loss is a constant value, whereas the power increases with frequency.

    However, there are two factors which also must be taken into account:

    - The increased voltage supplied to the coil may require an increased thickness of electrical insulation on the windings of the coil (and at other locations in the compressor). This may have a small effect on moving mass, and will also tend to reduce the amount of copper in the air gap, which will cause a decrease in motor efficiency.
    - The higher voltage requirement may lead to added mass and complexity with regard to the compressor power supply, control systems and also EMI issues.

- **Motor Losses.** Given that these are difficult to evaluate, and are very specific to the particular design of motor, these have not been analysed in detail, but should not be ignored in a real design. For a typical moving coil, permanent magnet motor they can be can be split into three categories:

    - Magnetic hysteresis. Some of the material in the magnetic circuit will experience a cyclic magnetic field, and the area enclosed by the ‘B-H’ curve undergone by the material represents a loss. This is typically a constant loss per cycle, so the power loss will be proportional to frequency.

  - The other two losses are similar to each other, and are difficult to separate out when a machine is being tested, they are both 'eddy current' losses:

    - 'Transformer' loss. AC current in any coil will induce currents in any closed loop of conductive material close to it, especially if there is good magnetic linkage. These losses are typically proportional to the square of current in the coil, and vary with the square of the drive frequency.

    - 'Eddy Current' Loss. This is caused by the motion of a conductor in the magnetic field (for instance a metallic 'coil former' move axially in an air gap). If the conductor consists of a closed loop, currents will flow, resulting in an i^2R loss. This induced current is proportional to the velocity, and overall these losses are also typically proportional to square of the induced current in the loop, and vary with the square of the drive frequency.

  At higher frequencies, the 'eddy current' losses are likely to be significant unless care is taken in the design of the motor and adjacent components.

  Note that the comments above apply to moving coil motors, but similar losses will exist in other designs of motor.

- **Structural Design.** Inertial (acceleration) forces within the moving components vary with the square of the operating frequency.

  - Hence any increase in frequency may require an increase in critical component dimensions in order to keep inertial stresses (or deflections) within acceptable limits. This will result in an increase in moving mass, which must be accounted for when calculating the resonant frequency.

  - Experience has shown that this is not an 'across-the-board' increase in mass, but is likely to be focussed in a few locations on some components.

  - If the goal of the exercise is to minimise size and mass, then there will typically be manufacturing limitations on components (i.e. it is difficult to machine a particular feature to less than 1 mm thickness). In this case the component, as designed for lower frequency operation, may still have plenty of 'margin' at higher frequencies.

- **Flow and Thermodynamic Losses.**
    - It is assumed that the cold head has been designed for the anticipated flow velocities.
    - Within the compression space, the ‘gas spring’ losses are taken into account elsewhere.
    - Within the compression space, the clearance seal loss is also accounted for elsewhere (these are likely to be independent of frequency).
    - It is assumed that the exit port from the compression space has been designed for the higher flows expected.

8.4 Simulation Results

The procedure outlined in section 8.2 was followed, the process being carried out in an Excel Spreadsheet.

The following parameters were fixed:

- Fill pressure 35 bar (absolute)
- Stroke of 12.8 mm (peak-to-peak).
- Gas Spring clearance seal length of 15 mm
- Gas spring clearance seal radial gap of 10 μm

The exercise was limited to a variation in the gas spring diameter and the ‘End Clearance’ (“D” and “L_e” in Figure 11), with the geometry as defined in that figure. The range of values considered for D and L_e were (units are mm):

- $35 \leq D \leq 80$
- $30 \leq L_e \leq 90$

Figure 12 shows how the characteristics of the gas spring vary with the ‘End clearance’; note the following:

- The end clearance defines the compression ratio in the gas spring; low clearance implies high pressure ratio and high peak-to-peak pressure.
- Higher peak-to-peak pressure will give a higher gas spring stiffness and a higher resonant frequency.
- The gas spring piston must be thicker to withstand the high pressures, so the piston mass increases at low values of End Clearance.

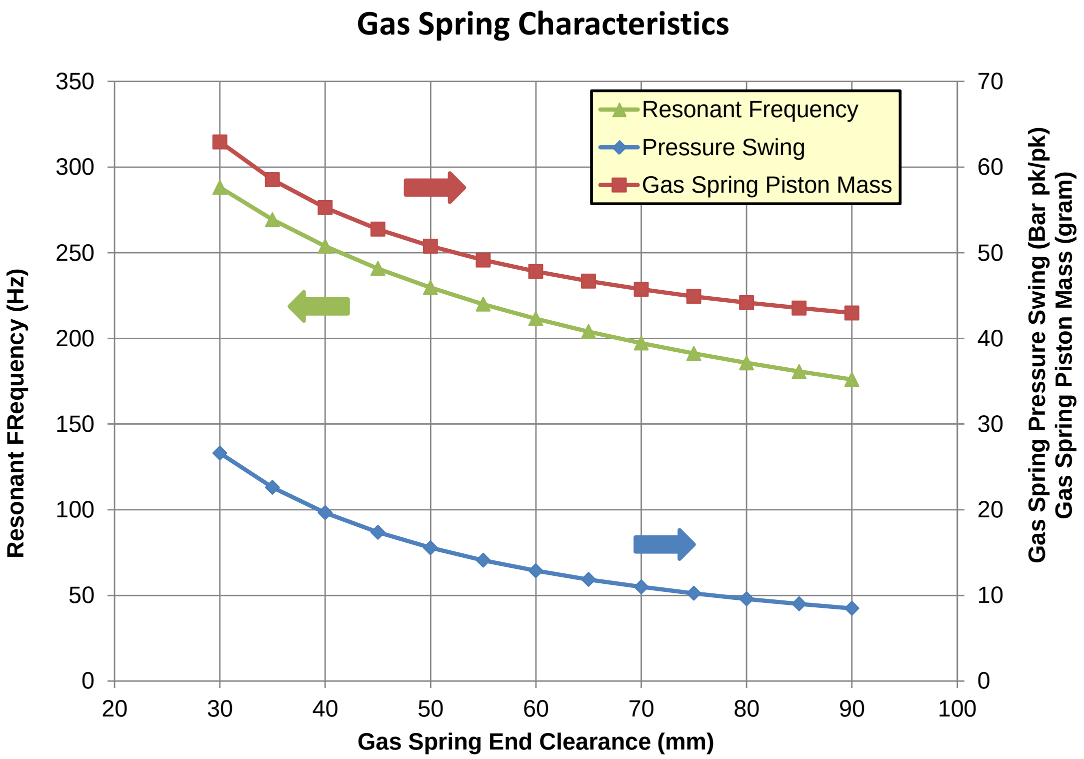

Figure 13 Gas Spring Characteristics as a function of End Clearance (gas spring diameter = 60 mm).

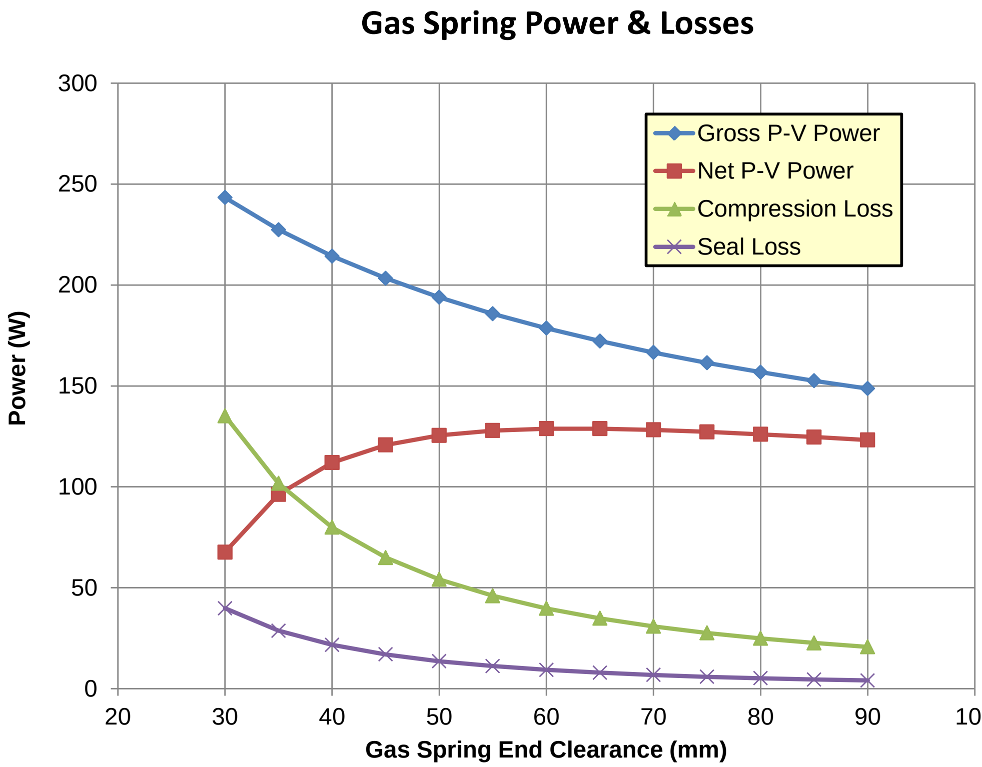

Figure 12. Gas Spring gross and net power, and losses, as a function of End Clearance (gas spring piston diameter = 60 mm).

Figure 13 shows the gross power, net power, and the gas spring losses as a function of the gas spring end clearance:

- The gross power is proportional to the frequency
- The Net Power is defined as

$$Net\ Power = Gross\ Power - Seal\ Loss - Compression\ Loss$$

- As stated above, at a low value of end clearance, the pressure swing increases.
- Both the compression loss and the clearance seal loss vary with the square of the pressure swing, so these are much higher at low values of end clearance.
- For this case, the net “*P-V* ” power available is at a maximum at an end clearance of about 60 mm (though the curve is fairly flat in this region).

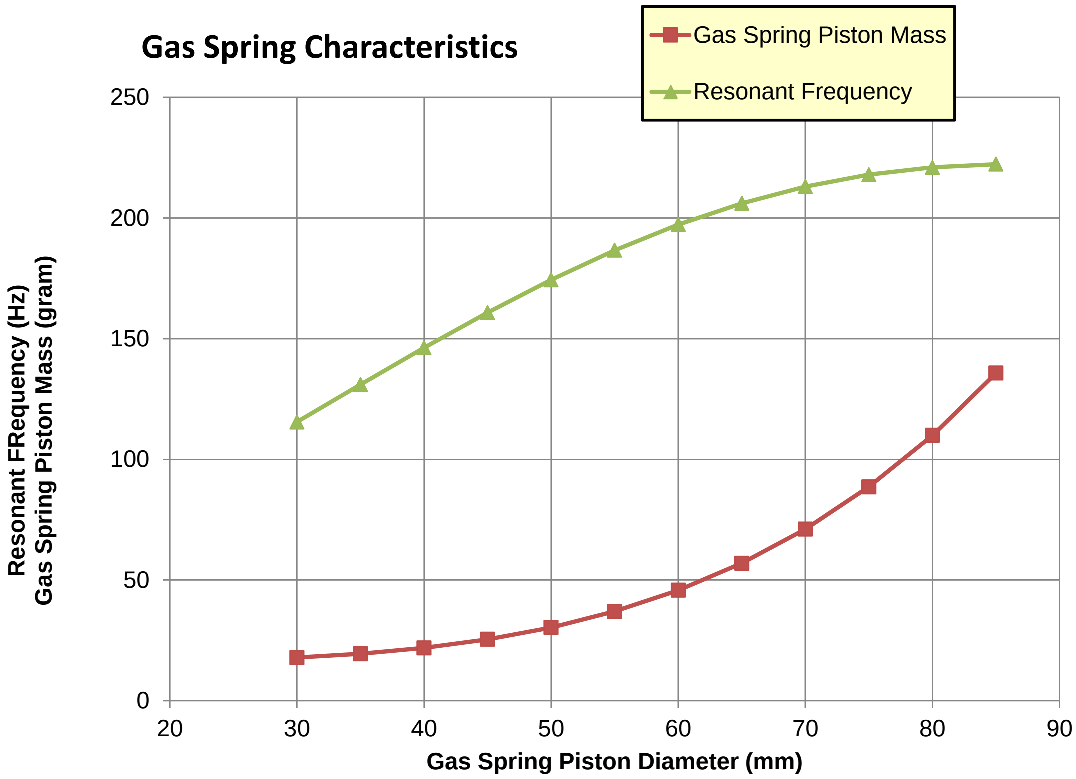

Figure 14. Resonant Frequency and gas spring mass as a function of Gas Spring Piston Diameter (End Clearance = 70).

Figure 14 shows the variation of resonant frequency and gas spring piston mass for a fixed End Clearance.

- As the gas spring piston diameter increases, the gas spring stiffness increases (Eq. 7), but the piston mass also increases.

- The pressure swing is constant, and is omitted from this graph.

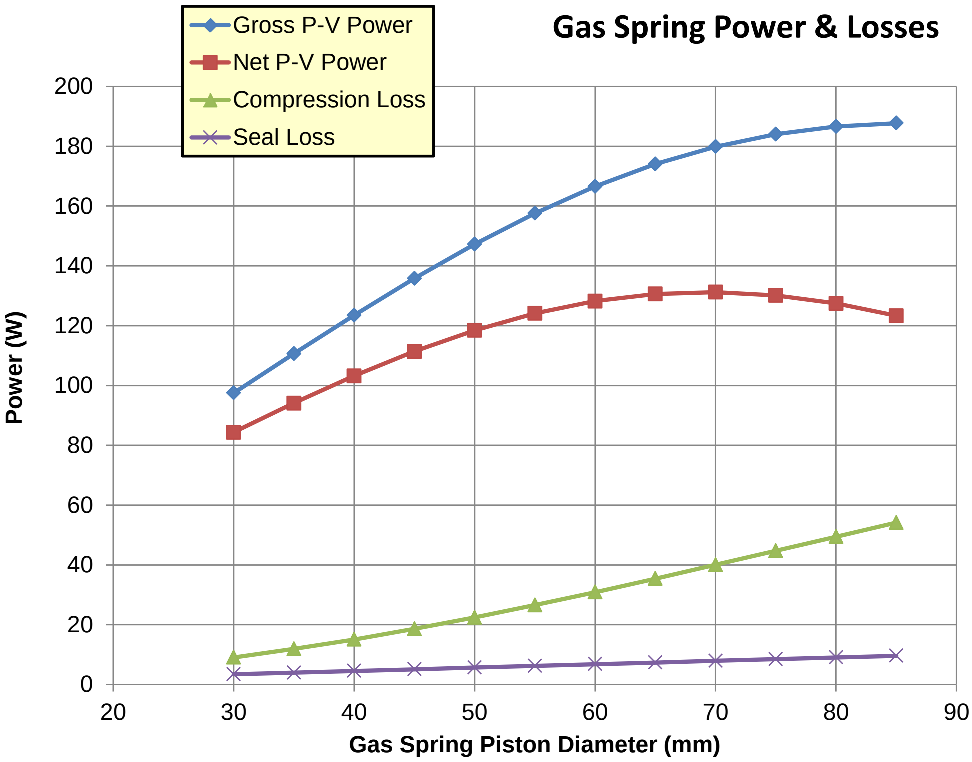

Figure 15. Gas Spring gross and net power, and losses, as a function of Gas Spring Piston diameter (gas spring end clearance = 60 mm).

Figure 15 shows the variation of power and losses with piston diameter.

- The gross power is proportional to frequency.

- The seal loss is proportional to piston diameter

- The compression loss increases with diameter

- The net power exhibits a peak at about 70 mm

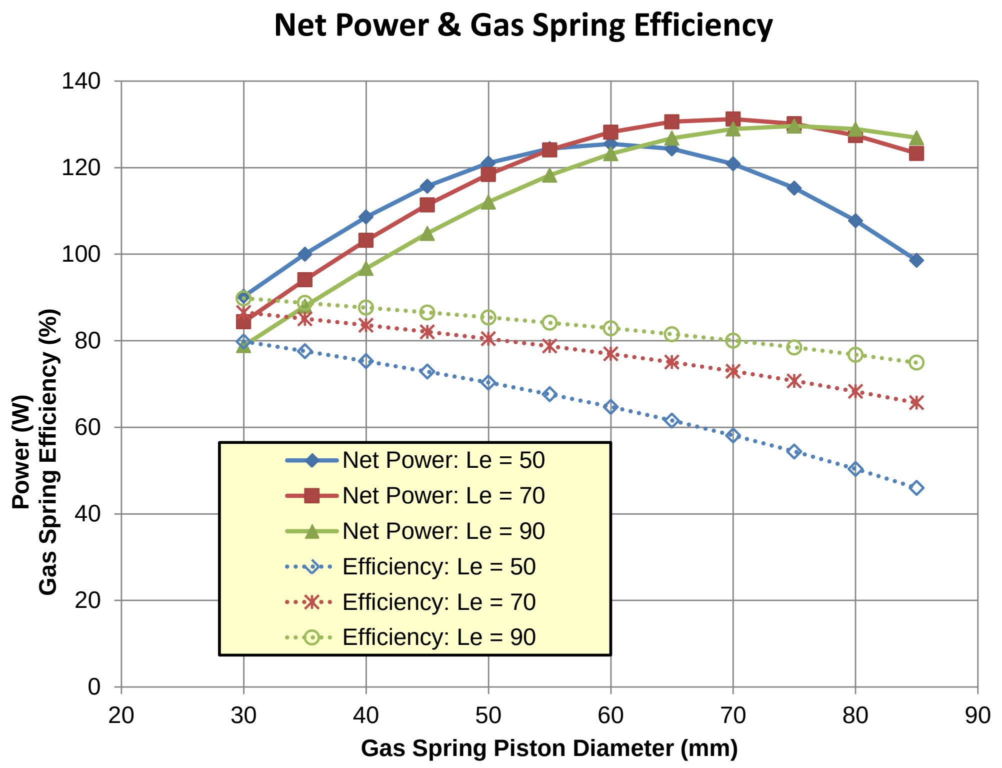

Figure 16. Net Power and Gas Spring Efficiency as a function of Gas Spring Piston Diameter and End Clearance.

Figure 16. Shows the Net Power and "Gas Spring Efficiency" over the range of variables considered above.

- This efficiency is defined as

$$Gas\ Spring\ Efficiency = \frac{Net\ Power}{Gross\ Power}$$

- The maximum value of net power does not vary much with the End Clearance
- The gas spring efficiency varies with End Clearance: larger end clearances are more efficient
- Note also that larger end clearances imply a larger compressor.
- It is possible to have different diameters for the gas spring piston and gas spring volume (i.e. not the geometry shown in Figure 11), and this would allow a shorter gas spring. Such a geometry would deviate from Kornhauser's assumptions so some caution would be needed when evaluating losses.

8.5 Summary of Simulation Results

The design of an auxiliary gas spring is a trade-off between increasing the frequency (and consequently the gross power) and the associated compression losses, which tend to increase with the square of the pressure swing, and therefore become more significant with the high gas spring rates needed for higher frequency operation.

Taking into account these losses, the net power out of the system does have a maximum at a certain frequency; in the analysis above, the maximum net power occurs at a frequency in the range between 195 and 230 Hz. However at this point of maximum power, the gas spring efficiency is between 65 and 79%, i.e. between 21% and 35% of the gross power is needed to overcome the gas spring losses. This is probably excessive for many applications.

Table 2. **Ambient Compressor With Gas Spring**

		Original	With Gas Spring
Power Piston Diameter	mm	18	18
Gas Spring Piston Diameter	mm		40
Gas Spring End Clearance	mm		90
Maximum Stroke	mm (peak-to-peak)	12.8	12.8
Design Frequency	Hz	50	131
Effective Moving mass	gram	120	141
Fill Pressure	bar (abs)	35	35
Pressure Swing (power piston)	bar (peak-to-peak)	5.75	5.75
Pressure Swing (gas spring piston)	bar (peak-to-peak)		8.5
Mechanical Spring Stiffness (axial; total)	N/m	3900	3900
Compressor Shaft (P-V) power (Gross)	W	42.3	110.4
Compression Loss (gas spring)	W		10.2
Seal Loss (gas spring)	W		2.7
Compressor Shaft (P-V) power (Net)	W	42.3	87.7
Motor Efficiency	%	80	80
Electrical Power Input	W	52.9	138
Overall Efficiency	%	80	63
Overall Compressor Length	mm	160	220
Increase in length	%		38%

If the system is designed to run at a lower frequency than that of ‘maximum net power’, then the gas spring loss will be correspondingly lower. For the particular compressor analysed in this example, a likely operating point has been chosen, and the compressor performance is tabulated on the previous page.

Note that a constant motor efficiency has been assumed – if the design strategy outlined in section 8.3 has been followed, then the motor i^2R loss should less, but eddy current and other losses will be higher. For this table, an overall efficiency has been defined as

$$Overall\ Efficiency = \frac{Net\ "P{-}V"\ Power\ Out}{Electrical\ Power\ In} \tag{46}$$

In this case the net power out has gone up by a factor of 2.08, while the input power has increased by a factor of 2.61

In terms of size, the addition of a gas spring will probably add about 60 mm to the total length of the compressor, providing that shape of the gas spring compression space makes full use of the overall compressor diameter. Hence the power output from the compressor can be approximately doubled for a 38% increase in volume (and a slightly smaller increase in mass).

9 Conclusions

This study has investigated the possibilities of increasing the operating frequency of cryocooler compressors.

The operating frequency of a compressor is dependent on the following:

- Moving Mass
- Mechanical Spring Stiffness
- Gas Spring Stiffness

It is assumed that the moving mass is already optimised, and there is little scope for further reduction.

The stiffness of the mechanical springs can be increased by optimising the following:

- Material
- Manufacturing process
- Surface Treatment
- Spring geometry
- Clamping details

Given the lack of detailed information about the design of proprietary cryocooler compressors, it is difficult to estimate the likely impact of these improvements. However given the relatively small proportion of total stiffness that is due to the mechanical springs, it is unlikely that the resonant frequency of the compressor can be increased by more than about 12% solely due to changes in mechanical spring design.

Provision of an auxiliary gas spring does provide the potential for a large increase in operating frequency, but there are associated losses which can be significant at higher frequencies.

A methodology is demonstrated for the simple evaluation of a gas spring, and this has been applied to an existing design of compressor. There is a wide spectrum of possible designs, but one has been evaluated which shows an increase in net compressor power by a factor of 2.08, while the input power has increased by a factor of 2.61 and the overall size of the compressor increased by a factor of 1.38.

This example has been based on the potential to increase the power of an existing design, but it is anticipated that these techniques can be used to design from scratch a compressor. If this is done, then the design goal will not be an increase in power, but an optimisation of the specific power (Power per unit mass or per unit volume).

It must be noted that in the design of compressor, there may be many other factors which might put an upper limit on the operating frequency. Some of the most significant of these are:

- Inertial stresses on the moving components
- Power supply and electrical insulation for higher voltage operation
- Electromagnetic losses such as eddy currents
- Cold head design
- Spring arm resonances

It is hoped that the design techniques outlined in this report can be used to produce smaller, high frequency cryocooler compressors.

10 Acknowledgments

We would like to thank Erin Pettyjohn of AFRL and Brad Thompson of EOARD for their support.

This effort was sponsored by the Air Force Office of Scientific Research, Air Force Material Command, USAF, under grant number FA8655-11-1-3032. The views and conclusions contained herein are those of the authors and should not be interpreted as necessarily representing the official policies or endorsements, either expressed or implied, of the Air Force Office of Scientific Research.

11 Appendix A. Cryocooler Frequency Data

Table 3. **Cryocooler Frequency Data** (ref. 1)

Manufacturer	**Model**	**Compressor Displacement (cm^3)**	**Frequency (Hz)**	**Max Input Power (W)**	**Frequency for plot (Hz)**
Astrium	10 K			185	
Astrium	20 K	7.2	35	105	35
Astrium	50-80 K	3	44	51.5	44
Astrium	80 K	1.8	40	30.5	40
Ball	ACTDP			270	
Ball	SB335			60	
Ball	SB235		36 to 44	267	40
Lockheed Martin	ACTDP		30	208	30
Lockheed Martin	High Cap		31	450	31
Lockheed Martin	IRAD		31	240	31
Lockheed Martin	High Cap/2		31	600	31
Lockheed Martin	IRAD PT		31	100	31
Lockheed Martin	GIFTS		54	142	54
Lockheed Martin	High Power Mini PT	2.1	60	76	60
Lockheed Martin	NASA Mini PT	1.6	60	15	60
Lockheed Martin	EM PT		54	95	54
Lockheed Martin	Coaxial Avionics PT		65	75	65
Lockheed Martin	JPL Gamma-Ray	2	42	30	42
Raytheon	RSP2 HC		40 to 55	512	47.5
Raytheon	RSP2 MC		40 to 55	234	47.5
Raytheon	RS1		43 to 49	115	46
Raytheon	DUC		45 to 65	77	55
Northrop Grumman	ACTDP			229	
Northrop Grumman	High-Cap	26	30	370	30
Northrop Grumman	HCC	26	30 to 55	570	42.5
Northrop Grumman	Micro	0.65	95 to 120	43	107.5
Northrop Grumman	Mini		> 80	80	80
Northrop Grumman	HEC		57 to 70	180	63.5
Northrop Grumman	HEC/2		57 to 70	147	63.5

- Some cryocoolers have a range of powers at different temperatures. The power quoted here is the largest of these.

- Where there is a range of frequencies given, the mean is used, except for the NG Mini, which is at the bottom limit

- Power input is to the ‘Thermo-Mechanical Unit’, and in some cases is estimated from the system input power.

12 Appendix B. Estimation of Gas Spring Piston Moving Mass

The addition of a gas spring to a compressor, of necessity, implies an increase in the effective moving mass. The increase in moving mass will tend to reduce the resonant frequency of the compressor; hence it is important to understand the relationship between the desired characteristics of the gas spring, the added mass, and the consequent change in frequency.

In a real design, there are many design decisions that need to be made with regard to any piston, including

- Operating frequency
- Operating stroke
    - Combining stroke and frequency gives a requirement for the inertial loading (peak acceleration) experienced by the piston
- Pressure swing
- Piston Diameter
- Method of attachment
- General shape
- Design of piston/cylinder seal
    - Minimum permissible piston/cylinder gap
- Material
    - Lifetime/maximum stress
- Environmental considerations:
    - Temperature range (operating & non-operating)
    - Launch vibration

For this exercise, the following criteria were imposed (see Figure 18):

- A fixed diameter for attachment of the piston to the moving structure of the cryocooler (28.5 mm)
- Variable diameter (“D” in Figure 18.)
- Seal Length of 22 mm
- ‘Cup’ type piston
- Base thickness equal to radial wall thickness (“T” in Figure 18).
- Maximum radial distortion of sealing surface 5 μm.

A drawing of the piston is shown in Figure 18 below. A solid model of the piston was then subject to an FE analysis as follows:

- The piston diameter was changed
    - Run FE model
    - Analyse results
    - If radial displacement is not equal to 5 μm then:
        - Change Value of wall thickness (“T” in Figure 18.); run the model again
    - When the maximum radial displacement is equal to 5 μm then record the mass.

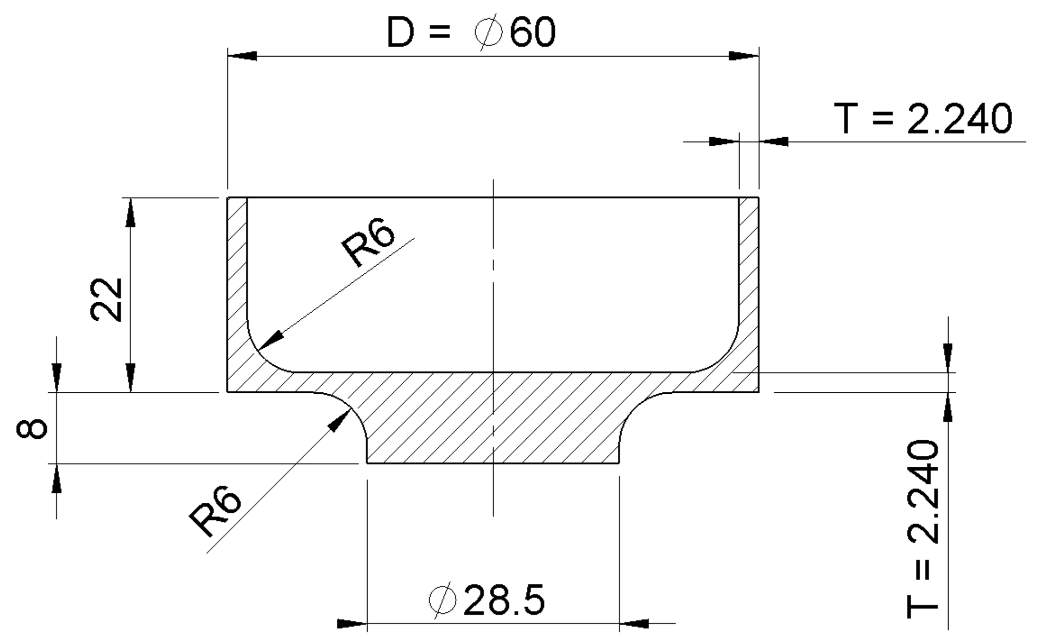
D = ∅60
T = 2.240
R6
22
8
R6
∅28.5
T = 2.240

Figure 17. Model for Gas Spring Piston mass estimate

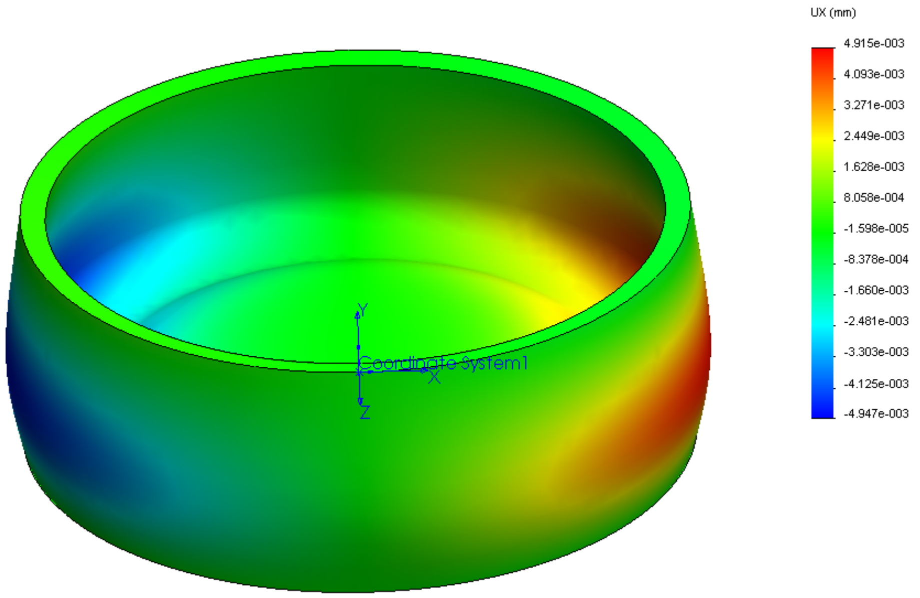
UX (mm)
4.915e-003
4.093e-003
3.271e-003
2.449e-003
1.628e-003
8.058e-004
-1.598e-005
-8.378e-004
-1.660e-003
-2.481e-003
-3.303e-003
-4.125e-003
-4.947e-003
Y
Coordinate System1
X
Z

Figure 18. Typical FE output from piston analysis. The plot shows displacement in the "X" direction only. Loading and displacement is actually axisymmetric, but if the total displacement is shown, the radial deformation (which is critical) is 'swamped' by the larger axial deformation (which is irrelevant for this exercise).

The results of this exercise are tabulated below, and also shown in Figure 19.

Table 4. **Gas Spring Piston Mass (grams)**

		Piston Diameter (mm)		
		40	**60**	**80**
Pressure Swing MPa (zero/peak)	**0.5**	21.7	43.58	96.09
	1.0	25.02	58.07	131.81
	2.0	30.4	76.87	226.55

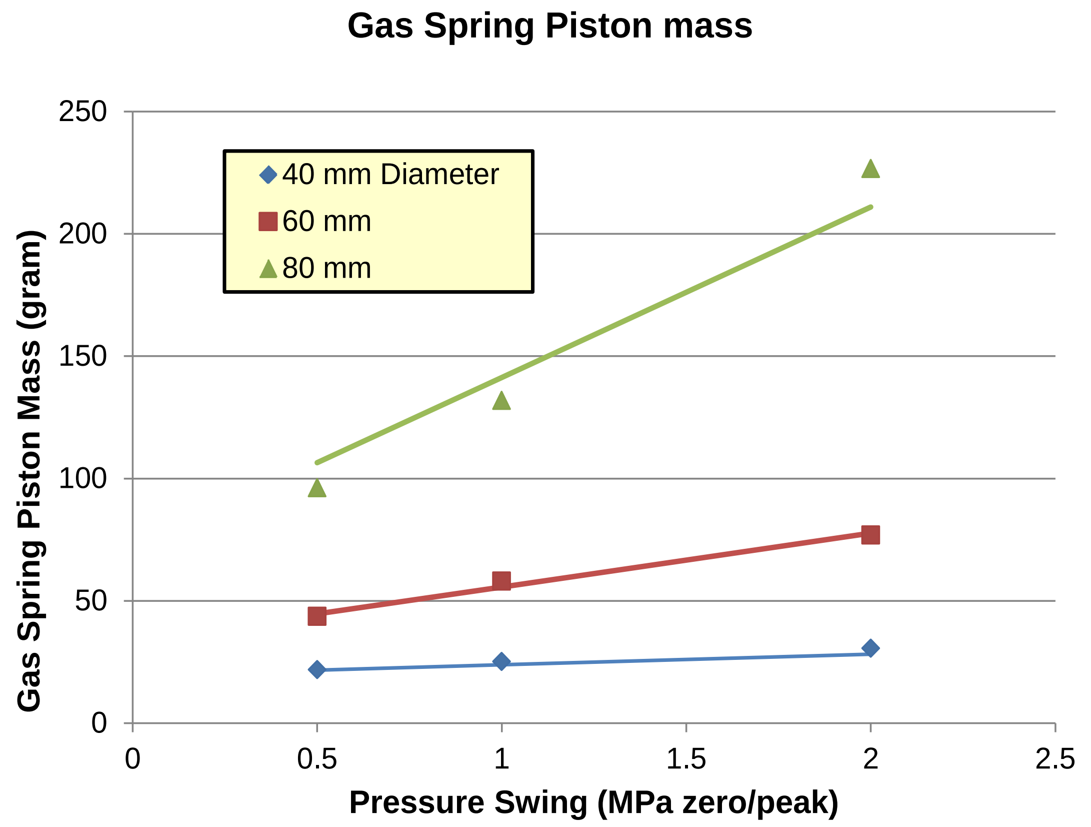

Figure 19. Mass of gas spring piston as a function of piston diameter and gas spring pressure amplitude. The lines are an approximate fit using equation (47) below.

The values in the table above were then subjected to a crude curve fitting exercise, with the following being a good approximation to the data:

$$m_{gp} = 16 + 1.7 \times 10^{-6}(0.8 + p_a)D^4 \tag{47}$$

Where

m_{gp} = estimated mass of gas spring piston (grams)
p_a = Gas spring pressure amplitude (zero-to-peak) (MPa)
D = Gas spring piston diameter (mm)

13 REFERENCES

---

1 Curran, D.G. et al, “Space Cryocooler Vendor Survey Update: 2007”, Aerospace Report No. TOR-2008(1033)-7691, Aerospace Corp, El Segundo, CA, USA, Jan 2008.

2 Bailey, P.B., Dadd, M.W., Cheuk, C.F., Hill, N.G., Raab, J., “Scaling of Cryocoolers 12, Kluwer Academic/Plenum Press, New York (2003), pp 247-253.

3 Wang, X, Dai, W., et al, “Performance of a Stirling-Type Pulse Tube Cooler for High Efficiency Operation at 100Hz”, Cryocoolers 16, ICC Press, Boulder, Co, USA, 2011, pp157-162.

4 Spoor, P.S., “Acoustic-Stirling 55 Gal/Day Oxygen Liquefier for Use on Aircraft Carriers”, Cryocoolers 15,, ICC Press, Boulder, Co, USA, 2009, pp 681-685

5 Bailey, P.B., Dadd, M.W., Stone, C.R., “Cool and Straight: Linear Compressors for Refrigeration”, Proc. Inst. R., 2010-2011. 4-1

6 Lee, K.P., “A Simplistic Model of Cyclic Heat Transfer Phenomena in Closed Spaces.” 18th IECEC, 1983.

7 Cooke-Yarborough E.H., Ryden, D.J., “Mechanical power losses caused by imperfect heat transfer in a nearly-isothermal Stirling engine.” SAE, 1985.

8 Kornhauser, A.A., Smith, J.L., “A Comparison of Cylinder Heat Transfer Expressions Based on prediction of Gas Spring Hysteresis Loss”, Fluid Flow in Heat Transfer and Reciprocating Machinery, pp 89 – 96, ASME 1987.

9 Bailey, P.B., Dadd, M. W., Reed, J.S., Stone, C.R., Davis, T., “Gas Spring Losses in Linear Clearance Seal Compressors”, Cryocoolers 14, ICC Press, Boulder, Co, USA, 2007, pp 345-352.

10 Lekić, U., “Fluid Flow and Heat Transfer in a Helium Gas Spring – Computational Fluid Dynamics and Experiments”, doctoral dissertation, Univeristy of Twente, Nov 2011.

11 Walker, G., Senft, J. R., “Free Piston Stirling Engines”, Springer-Verlag, Berlin, 1985, pp118.

12 Green RH, Bailey PB, Roberts L, Davey G. The Design and Testing of a Stirling Cycle Domestic Freezer. Proc. of Conference on Applications for Natural Refrigerants, held in Aarhus, Denmark, 1996; International Institute of Refrigeration, France, 1996.